UNIVERSITY OF CALIFORNIA, SAN DIEGO

Genetic Screening for Novel mRNA Localization Factors in *Drosophila melanogaster*

A thesis submitted in partial satisfaction of the

requirements for the degree Master of Science

in

Biology

by

Juliana Chang

Committee in charge:

Professor James E. Wilhelm, Chair
Professor Gentry Patrick
Professor David Traver

2010

ProQuest LLC
789 East Eisenhower Parkway
P.O. Box 1346
Ann Arbor, MI 48106-1346

The Thesis of Juliana Chang is approved and it is acceptable in quality and form for publication on microfilm and electronically:

_____

_____

_____

Chair

University of California, San Diego

2010

TABLE OF CONTENTS

LIST OF FIGURES

LIST OF TABLES

ACKNOWLEDGEMENTS

I would like to express my sincere gratitude to my advisor Dr. James Wilhelm for providing me with the opportunity to complete my Master of Science thesis in his lab and for his continual guidance and assistance. I would also like to thank the members of the Wilhelm Laboratory for their encouragement, support, assistance and knowledge. In addition, I would like to thank my parents and family for their concern and encouragement throughout this project. Lastly, I would like to thank Dr. Traver and Dr. Patrick for serving as committee members for my thesis.

ABSTRACT OF THE THESIS

Genetic Screening for Novel mRNA Localization Factors in *Drosophila melanogaster*

by

Juliana Chang

Master of Science in Biology

University of California, San Diego, 2010

Professor James E. Wilhelm, Chair

Trailer hitch (tral) is a component of a ribonucleoprotein (RNP) complex that localizes to the endoplasmic reticulum (ER) in the egg chamber nurse cells of the *Drosophila melanogaster* oocyte (Wilhelm et al., 2005). Mutating *tral* results in

disruption of ER exit site distribution, which leads to defects in the trafficking of Gurken (Grk) a factor required for dorsal-ventral patterning, and Yolkless (Yl), the vitellogenin receptor. Both Grk and Yl accumulate in the oocyte and during late development Grk localizes to the dorsal-anterior region while Yl goes to the plasma membrane. However, when there is a *tral* loss of function, both proteins remain in the ER, which implies that *tral* is involved in secretion through the formation and organization of ER exit sites (Wilhelm et al., 2005). Identifying the mRNA targets of *tral* and genes that genetically interact with *tral* will help further our understanding of the role of *tral* in the secretory pathway. Therefore, a broad genetic screen was conducted to determine and locate genes that interact with *tral.*

INTRODUCTION

In an adult *Drosophila* ovary, there are 14-16 ovarioles each with a germanium at its tip, which give rise to cells that assemble into egg chambers (Lehmann et al., 1998). Egg chambers consist of 16 interconnected cells surrounded by a layer of follicle cells. Of this 16 cell cluster, one will become the oocyte while the other 15 cells become the nurse cells (King et al., 2005). The nurse cells will grow and accumulate yolk material and provide nutrients for the embryo. In addition, nutrients and developmental control elements move from the nurse cells to the oocyte. Following germline stem cell division, one daughter cell remains at the tip of the germanium while the other moves away from the tip to become a cytoblast, which undergoes division to produce a 16-cell germline cyst. During oogenesis stages 8 and 9, nurse cells will grow and accumulate yolk material. Follicle cells will migrate over the surface of the egg chamber at stage 9, leaving only a few follicle cells over the nurse cells (Xi et al., 2003).

Drosophila oogenesis requires the developing oocyte to become polarized along the anterior/posterior and dorsal/ventral axes. This is determined by cytoskeletal organization and distribution of specific mRNAs and proteins (MacDonald et al., 2007). The anterior-posterior axis is determined through the localization of two mRNAs to the anterior and posterior pole of the oocyte (van Eeden and St. Johnston, 1999; Riechmann and Ephryssi, 2001). *Bicoid (bcd)* mRNA is localized to the anterior of the oocyte and is translated to generate the homeodomain transcription factor that patterns the head and thorax of the embryo (Driever, 1993). *Oskar (osk)* mRNA, on

the other hand, first localizes in the anterior pole of the oocyte during stages 7 and 8 before localizing to the posterior of the oocyte during stages 9 and 10 (Wilhelm et al., 2003). It is responsible for directing the formation of the pole cells and abdominal determinants (Ephrussi et al., 1991; Kim-Ha et al., 1991; Ephrussi and Lehmann, 1992).

Localization of both *bcd* and *osk* mRNAs depend on reciprocal signaling between the oocyte and the overlying somatic follicle cells. During the early stages of oogenesis, a microtubule organizing center (MTOC) is found at the posterior end of the oocytes and nucleates microtubules that extend through the nurse cells (Theurkaurf et al., 1992). During later stages, Grk protein causes certain somatic follicle cells to adopt a posterior fate. Grk, a TGF-α like receptor, activates *Drosophila* EGF receptor in dorsal follicle cells (Macdonald et al., 2007, Roth et al., 2001). These cells then signal back to the oocyte to induce the disassembly of the posterior MTOC, leading to the formation of an anteroposterior gradient of microtubules (St. Johnston et al., 2003).

In addition to regulating cytoskeletal organization in early oogenesis, Grk also plays a central role in defining the dorsal ventral axis. Unlike *bcd* and *osk* mRNAs, *grk* mRNA is transported along the microtubule cytoskeleton to the dorsal-anterior region of the oocyte (Neuman-Silberberg and Schupbach, 1993). This localization confines the Grk protein to the dorsal-anterior ER-Golgi units, where local secretion will instruct the dorsal follicle cells to assume a dorsal cell fate. Follicle cells that have assumed a dorsal fate generate a specialized egg shell structure, the dorsal appendage,

which provides a useful marker of dorsal-ventral polarity in the early egg. As a consequence of its dual roles in regulating microtubule organization early in oogenesis and establishing dorsal ventral polarity in wild type egg chambers, Grk protein is homogenously expressed throughout the oocyte during stages 6-7 and then found in small puncta near the plasma membrane, which coincide with ER exit sites in the dorsal anterior region of the oocyte during stages 8-10 (Wilhelm et al., 2005).

tral, which is part of a RNA complex, is a gene required for efficient secretion of Grk, a dorsal-ventral patterning factor, to dorsal-anterior ER-Golgi units and Yl, a vitellogenin receptor to the plasma membrane. The Tral RNP complex localizes to subdomains of the ER that border the ER exit sites, and furthermore, *tral* has been found to be required for normal ER exit site formation. In addition, in *tral* mutants, abnormally large Grk puncta observed, suggesting that *tral* mutations disrupt Grk trafficking through a secretory pathway (Wilhelm et al., 2005).

One group identified that a P element insertion in the first intron of *tral*, KG08052, exhibited defects in the dorsal-ventral patterning of the eggshell (Bellen et al., 2004). Though various insertions and deletions of the gene, it was possible to generate different hypomorphic alleles of the *tral* mutants. 80% of the eggs laid by females homozygous for the KG08052 insertion displayed no dorsal appendages or a single fused appendage, a phenotype indicating ventralization of the eggshell. From this, it can be concluded that the disruption of *tral* is responsible for dorsal-ventral patterning defect in *Drosophila* (Wilhelm et al., 2005).

Findings have been published indicating that *tral* has a direct role in promoting efficient trafficking through the secretory pathway. However, to further understand *tral* and its effect on protein trafficking, a large genetic interaction screen was performed to identify novel genes that interact with *tral.* Further analysis of the genes identified from the screen and their relationship with *tral* can illustrate the connection between oogenesis and trafficking through the secretory pathway.

MATERIALS AND METHODS

Drosophila Cultures

Fly stocks were cultured at 20°C-25°C on standard food. Fly stocks were obtained from the Bloomington Stock Center at Indiana University.

Deficiency Crosses

Deficiency stocks obtained from the Bloomington Stock Center at Indiana University were crossed with weak, null and strong alleles of *tral* as shown below.

1) $\frac{\text{w; Tral}^{KG8052}}{\text{TM3, Sb}}$ Virgin females X $\frac{\text{Deficiency \#}}{\text{TM3, Sb}}$ males

2) $\frac{\text{w; Tral}^{D4}}{\text{TM3,Sb}}$ Virgin females X $\frac{\text{Deficiency \#}}{\text{TM3, Sb}}$ males

3) $\frac{\text{w; Tral}^{e03082}}{\text{TM3, Sb}}$ Virgin Females X $\frac{\text{Deficiency \#}}{\text{TM3, Sb}}$ males

Non-stubble females (w; Deficiency #/Tral^{KG8052}, w; Deficiency#/$\text{Tral}^{\Delta 4}$; w; Deficiency#/Tral^{e03082}) were collected from the above crosses to test for enhancement or suppression of the tral dorsal appendage phenotype. The progeny collected were then crossed with yellow white (yw) males and eggs were collected on grape agar plates. The eggs were then examined under a microscope to score for dorsal appendage defects.

Processing and transformation of clone for LD10322

cDNA was obtained from Drosophila Genomic Resource Center, Bloomington, IN. Their protocol for DNA recovery was used to obtain the cDNA: 50µl of 1X sterile TE was added to a microfuge tube containing the DNA from a cDNA clone of the CG16718 gene on a Whatman FTA disc. The solution was quickly pipetted up and down twice before the TE was removed and the tube was placed on ice. 50µl of One Shot Top 10 Chemically Competent *E. coli* cells was added and then heat shocked for 2 minutes at 42° Celsius. The cells were then transferred to 1ml of LB media and incubated for an hour on the shaker at 37 ° Celsius. Afterwards, 200µl of the solution was plated on LB + ampicillin plates that were placed upside down at 37° Celsius overnight.

Making Sense and Anti-sense 500 base pair CG16718 probes and *osk* probes

The cDNA clone that was minipreped using Invitrogen Purelink Quick Plasmid Miniprep Kit was digested with XhoI and EcoRI restriction enzymes (New England Biolabs). To generate the *osk* and 500 base pair (bp) CG16718 sense and antisense probes located 660 bp into the CG16718 gene for *in situ* hybridization experiments, transcription reactions were performed. An Sp6 promoter was added to the beginning of the sense strand, which served as a control, while a T7 promoter was added to the anti-sense strand. For the sense strand, 1µg of DNA (obtained either from the restriction digest or the from the Novagen KOD PCR reaction), 2µl of Roche Biotin 10 X Mix, 2µl 10 X Roche Transcription Buffer, 2µl Roche Sp6 RNA Polymerase and water were mixed together to create a 20µl reaction at room

temperature. To generate the anti-sense strand, 1µg of DNA, 2µl of Biotin 10 X Mix, 2µl 10 X Roche Transcription Buffer, 2µl Roche T7 RNA Polymerase and water were added together to create a 20µl mixture at room temperature. Then the tubes were quickly mixed and centrifuged before being incubated for 3 hours at 37 ° Celsius. 2µl of Invitrogen RNAse free DNAse was added to the solution and then the mixture was incubated at 37 ° Celsius for 30 min. 1µl of 0.5M EDTA pH 8.0 that had been anti-nuclease treated was then added and 1µl of the mixture was run on a TBE gel in TBE buffer to confirm that the transcription reaction worked properly.

Acetone *in situ* hybridizations

Ovaries were dissected in room temperature Grace's media (Gibco) and fixed at room temperature for 20 minutes in 200µl PBSF (4% formaldehyde in PBS), 2µl 10% Tween 20 and 600µl heptane. The heptane phase was removed and 500µl of PBSF and 10µl 10% Tween 20 was added and the ovaries were fixed for 5 minutes at room temperature. The PBSF layer was then removed and the ovaries were rinsed with 1 ml methanol twice. The ovaries were stored in 1 ml methanol at -20° Celsius for at least 24 hours before in situ hybridizations were performed.

Ovaries prepared as described above were then washed with methanol twice for 5 min on the shaker. Then the ovaries were washed in a 3:1 ratio of methanol and water solution for 5 minutes, a 1:1 ratio of methanol and water for 5 minutes and then a 1:3 Methanol and water solution for 5 minutes, respectively at room temperature.

The ovaries were then washed in water for 5 minutes and then treated with 80% Acetone for 10 minutes at minus 20 ° Celsius.

Ovaries were then washed in PBS with 0.1% Tween 20 (PBTwx) twice for 5 minutes at room temperature on a shaker before being fixed in PBTwx and 4% Formaldehyde for 25 minutes at room temperature on a shaker. The ovaries were then rinsed in PBTwx four times for 5 minutes each at room temperature. The PBTwx was replaced with a 15 minute wash of equal amounts of PBT and hybridization buffer (50% formamide, 20 X SSC, 10 mg/ml salmon sperm DNA, 50 mg/ml heparin, 50 mg/ml tRNA, 10% Tween 20 and RNAse free water) for 15 minutes at room temperature. Afterwards, the ovaries were incubated in hybridization buffer for 30 minutes twice at 55° Celsius and then hybridized overnight at 55° Celsius with the sense and antisense CG16718 and *osk* probes.

After hybridization, the ovaries were washed through the following series at 55° Celsius: 1x 5 minutes 1000 µl pre-warmed hybridization buffer, 2X 30 minutes 1000 µl pre-warmed hybridization buffer. The solution was then replaced with 50 PBTwx: 50 Hybridization buffer for 10 minutes before a quick wash in PBTwx and then 3 washes for 5 minutes each wash in PBTwx on a shaker at room temperature. The ovaries were then treated in 1% Hydrogen peroxide for 20 minutes at room temperature and then washed three times in PBTwx for 5 minutes each time on a shaker at room temperature. Then, the ovaries were blocked in PBTwx and 1X Blocking reagent for 30 minutes at room temperature. Afterwards, the ovaries were

incubated overnight in foil in the primary antibody streptavidin-HRP that was diluted 1:100 in PBTwx and blocking reagent.

The next day, the ovaries were first washed in PBTwx briefly before being washed in PBTwx for 15 minutes three times. The ovaries were then incubated in a tyramide solution, which was diluted 1:50 in Amplification buffer in foil for 30 minutes. The ovaries were then briefly washed in PBTwx and then washed again in PBTwx for 10 minutes before a drop of Vectashield was added to the ovaries and then were either place in 4 ° Celsius or mounted on slides in preparation to be viewed using the Leica Sp5 confocal microscope.

Antibody Staining

In preparing the ovaries for antibody staining, the dissections were prepared according to the protocol as previously described for *in situ* hybridization. The ovaries were dissected in Grace's media, then fixed with 200µl Grace's with 4% formaldehyde and 50µl of heptane for 10 minutes, shaking at room temperature. The samples were quickly rinsed in PBT (PBS + 0.2% TritonX-100) and then washed in PBT for 20 minutes, shaking at room temperature. They were then incubated in blocking solution (PBT+ 5% BSA + 0.02% Sodium Azide), shaking, for 30 minutes at room temperature before being incubated in α-cap 'n' collar (rabbit, 1:100 dilution in blocking solution) shaking overnight at 4 ° Celsius. The ovaries were washed for 4 times 30 minutes each in blocking solution, The samples were incubated in Alexa Fluor 488 goat anti-rabbit IgG (H+L) (Invitrogen) at a dilution of 1:100 in blocking

solution and covered in foil on a shaker at room temperature. Afterwards, the ovaries were incubated with DAPI at a dilution of 1:5000 in PBT for 5 minutes in foil on a shaker at room temperature before being washed overnight at 4 ° Celsius in PBT. The ovaries were then incubated for 20 minutes in Phallodin (1:200) in PBT on a shaker at room temperature in foil. The samples were then quickly rinsed three times in 1X PBS and mounted in Vectashield for observation using the Leica TCS SP2 confocal microscope. The cap 'n' collar antibody was a gift from Dr. William McGinnis at the University of California, San Diego.

RESULTS AND DISCUSSION

Genetic Screen

The Bloomington Drosophila Stock Center at Indiana University generated fly stocks where defined segments of the genome have been deleted. Using these deficiency stocks, it was possible to perform a broad genetic screen to identify a general region of the chromosome that contains several genes, one of which might interact with the gene in question. By using the third chromosome deficiency collection, which covers 98% of the third chromosome, a screen was performed to identify interactions with *tral,* which is also found on the third chromosome.

tral homozygous mutants have eggs with fused or missing dorsal appendages instead of the normal eggshell phenotype of two distinct dorsal appendages (Figure 1). Heterozygous tral mutants do not display this phenotype. However, we hypothesized that introducing other mutations into the tral heterozygous background could result in the fused dorsal appendage phenotype, uncovering a genetic interaction. To determine which genes genetically interact, tral was crossed with a variety of deficiency stocks. To determine the severity of the defect, the dorsal appendages and hatching rates of the eggs from the crosses described above were counted on a grape agar plate. Egg counting is a quantitative process where weak mutations can be easily picked up and the severity of the dorsal-ventral patterning defect can be scored depending on whether 2, 1 or 0 appendages are present. Genes that ineracted strongly with tral would result in embryos with the same dorsal appendage defects seen in homozygous tral mutants.

To uncover the regions on the third chromosome that interact with *tral,* the deficiency stocks were crossed with null, strong and weak alleles of *tral* (Wilhelm et al., 2005*)*. $tral^{KG08052}$ and $tral^{e03082}$ are weak and strong hypomorphic alleles of *tral*, respectively, while $tral^{\Delta 4}$ is a null mutation. Therefore, it is expected that the dorsal appendage defect would be least noticeable in $tral^{KG08052}$ and greater with $tral^{e03082}$. Since $tral^{\Delta 4}$ is a null mutation, it would be expected that the dorsal appendage defect would be greatest with crosses with the $tral^{\Delta 4}$ allele (Table 1, Table 2 and Table 3).

To determine which of the genes altered in a specific deficiency stock genetically interacted with *tral,* the affected region was analyzed to subregions of the deficiency that also interact with the different alleles of *tral*. Then, these deficiency stocks were crossed with the three alleles of *tral.* Using this data (Table1, Table 2 and Table 3), regions could be ruled out or identified as having a genetic interaction with *tral* depending on if these stocks had high dorsal appendage formation defects or not (Figure 4-15 and Table 5-13). From this genetic screen, fifteen deficiency stocks were found to have a strong interaction with *tral* (Table 4) and four genes were specifically analyzed.

Wilhelm et. al, 2005

Figure 1. (A) Two normal dorsal appendages present on eggs from yw females. $tral^{KG08052}$, $tral^{e03082}$, $tral^{D4}$ females lay ventralized eggs with either (B) one fused dorsal appendage or (C) no dorsal appendages.

Table 1. Dorsal Appendage Defect for deficiency stocks from the third chromosome crossed with $tral^{KG08052}$

Genotype	Sequence Coordinates	Eggs screened	Abnormal Appendage eggs	% of Abnormal Appendages	Hatching Rate	Hatching %
Df(3L)ED4515	3L:13,932,272..14,030,132	416	2	0.5%	343/416	82.5%
Df(3L)ED4529	3L:13,932,272..14,070,123	546	5	0.9%	139/159	87.4%
Df(3L)ED4528	3L:14,030,141..14,070,123	335	1	0.3%	131/145	90.3%
Df(3L)ED4534	3L:14,030,141..14,186,794	257	0	0.0%	213/257	82.9%
Df(3L)ED4978	3L:21,526,907..21,873,785	110	3	2.7%	106/110	96.4%
Df(3L)ED230	3L:22,127,751..22,827,471	260	5	1.9%	207/260	79.6%
Df(3L)ED231	3L:22,864,916..22,938,620	196	12	**6.1%**	184/196	93.9%
Df(3L)ED4413	3L:8,759,532..8,972,087	331	2	0.6%	302/331	91.2%
Df(3R)ED5156	3R:1,090,655..1,284,574	300	0	0.0%	385/430	89.5%
Df(3R)Exel6144	3R:1,328,532..1,438,438	351	2	0.6%	295/351	84.0%
Df(3R)ED5177	3R:1,426,351..1,449,817	403	9	2.2%	285/403	70.7%
Df(3R)Exel7283	3R:1,474,083..1,572,402	273	7	2.6%	190/273	69.6%
Df(3R)ED5197	3R:1,474,504..1,833,866	300	0	0.0%	200/300	66.7%
Df(3R)ED5196	3R:1,510,301..1,833,866	503	24	**4.8%**	367/471	77.9%
Df(3R)Exel6145	3R:1,542,490..1,638,975	456	3	0.7%	289/456	63.4%
Df(3R)ED5020	3R:107,408..216,113	170	2	1.2%	130/170	76.5%
Df(3R)ED5092	3R:107,408..912,807	5	0	0.0%	0/5	0.0%
Df(3R)ED5911	3R:14,568,649..14,991,505	187	2	1.1%	138/187	73.8%
Df(3R)ED5938	3R:14,732,356..15,467,758	221	3	1.4%	169/221	76.5%
Df(3R)ED5942	3R:15,052,016..15,660,809	624	23	3.7%	487/624	78.0%
Df(3R)Exel6184	3R:15,289,185..15,467,038	171	9	**5.3%**	180/271	66.4%
Df(3R)ED6025	3R:15,468,450..16,135,24	431	3	0.7%	255/339	75.2%
Df(3R)ED6027	3R:15,662,595..16,135,241	546	13	2.4%	372/481	77.3%

Table 1. Dorsal Appendage Defect for deficiency stocks from the third chromosome crossed with $tral^{KG08052}$ (continued)

Df(3R)Exel6185	3R:16,135,245..16,376,386	347	6	1.7%	238/347	68.6%
Df(3R)ED6058	3R:17,122,217..17,545,322	205	1	0.5%	168/205	82.0%
Df(3R)ED6076	3R:17,459,227..17,868,550	528	13	2.5%	361/528	68.4%
Df(3R)ED6090	3R:17,867,946..18,524,141	409	0	0.0%	282/409	68.9%
Df(3R)ED6091	3R:18,413,403..18,552,029	726	10	1.4%	640/726	88.2%
Df(3R)ED6096	3R:18,413,403..19,047,691	195	3	1.5%	177/195	90.8%
Df(3R)ED6103	3R:18,724,275..19,084,137	140	1	0.7%	134/140	95.7%
Df(3L)ED5017	3R:18,724,275..22,991,401	790	16	2.0%	326/568	57.4%
Df(3R)ED7665	3R:2,916,249..3,919,805	200	2	1.0%	199/200	99.5%
Df(3R)ED6232	3R:21,862,598..22,624,704	599	0	0.0%	556/599	92.8%
Df(3R)ED6265	3R:22,937,981..23,405,492	110	1	0.9%	107/110	97.3%
Df(3R)ED6242	3R:22,966,066..23,089,591	200	7	3.5%	165/200	82.5%
Df(3R)ED6310	3R:24,964,617..25,337,875	593	8	1.3%	520/593	87.7%
Df(3R)Exel6212	3R:25,040,897..25,113,953	420	4	1.0%	291/420	69.3%
Df(3R)ED6316	3R:25,081,04..25,608,38	390	15	3.8%	335/390	85.9%
Df(3R)ED5142	3R:279,018..1,090,605	390	1	0.3%	310/390	79.5%
Df(3R)ED5223	3R:3,317,426..3,919,805	513	9	1.8%	187/513	36.5%
Df(3R)ED5230	3R:3,803,496..4,478,856	314	4	1.3%	293/314	93.3%
Df(3R)ED5330	3R:4,495,308..5,055,517	211	4	1.9%	152/211	72.0%
Df(3R)ED5331	3R:4,859,916..5,055,517	244	7	2.9%	123/197	62.4%
Df(3R)ED5095	3R:475,607..912,807	335	2	0.6%	265/335	79.1%
Df(3R)ED5327	3R:5,052,798..5,055,517	282	11	3.9%	217/282	77.5%
Df(3R)ED5428	3R:5,456,513..5,874,333	223	2	0.9%	22/166	1.2%
Df(3R)ED5438	3R:5,552,399..5,874,333	143	0	0.0%	100/143	69.9%
Df(3R)ED5454	3R:5,552,399..5,937,180	285	0	0.0%	175/285	61.4%
Df(3R)ED5474	3R:5,935,134..6,176,446	268	4	1.5%	226/268	84.3%
Df(3R)ED5472	3R:5,996,223..6,176,446	521	5	1.0%	235/521	45.1%
Df(3R)ED5506	3R:6,710,720..6,998,470	427	2	0.5%	310/427	72.6%
Df(3R)ED5518	3R:6,710,720..7,445,622	244	1	0.4%	166/244	68.0%
Df(3R)ED5138	3R:606,794..1,090,605	412	19	**4.6%**	119/295	40.3%
Df(3R)ED5516	3R:7,059,89..7,445,622	217	4	1.8%	165/317	52.1%
Df(3R)Exel6143	3R:776,726..912,504	372	0	0.0%	254/372	68.3%
Df(3R)ED5554	3R:8,106,835..8,269,738	272	0	0.0%	234/272	86.0%
Df(3R)ED5591	3R:8,176,253..8,545,732	471	5	1.1%	367/465	78.9%
Df(3R)ED5610	3R:8,269,738..8,821,397	568	3	0.5%	282/568	49.6%
Df(3R)Exel6185	3R:16,135,245..16,376,386	347	6	1.7%	238/347	84.4%
Df(3R)ED6058	3R:17,122,217..17,545,322	205	1	0.5%	168/205	68.6%
Df(3R)ED6076	3R:17,459,227..17,868,550	528	13	2.5%	361/528	82.0%
Df(3R)ED6090	3R:17,867,946..18,524,141	409	0	0.0%	282/409	68.4%
Df(3R)ED6091	3R:18,413,403..18,552,029	726	10	1.4%	640/726	68.9%

Table 1. Dorsal Appendage Defect for deficiency stocks from the third chromosome crossed with $tral^{KG08052}$ (continued)

Df(3R)ED5613	3R:9,085,471..9,470,856	336	10	3.0%	201/224	89.7%
Df(3R)ED5622	3R:9,509,544..9,809,634	448	3	0.7%	335/448	74.8%
Df(3R)ED5634	3R:9,843,625..10,103,665	625	0	0.0%	417/625	66.7%
Df(3R)ED5644	3R:9,843,625..10,451,431	206	1	0.5%	182/206	88.3%
Df(3R)ED5147	3R:912,842..1,193,526	250	8	3.2%	186/250	74.4%

The KG08052 insertion site lies within the first intron of *tral* and is considered to be a weak hypomorphic allele (Wilhelm et al., 2005). Therefore, if the deficiencies used in the genetic screen experiments interacted with this allele of *tral*, a slight dorsal-ventral patterning defect would have been observed. Deficiencies that led to higher than expected dorsal appendage defects with the $tral^{KG08052}$ included Df(3R)ED5138, Df(3R)Excel6184, Df(3R)ED5196 and Df(3L)ED231. To determine more accurately if deficiencies truly interacted with *tral,* other alleles of *tral* were crossed with the deficiency stocks to verify the possible interactions. The results presented in Table 1 must be taken into account with the data present in Table 2 and Table 3. When the deficiency stock is crossed with only one allele of *tral*, it cannot be accounted for as to how much of the dorsal appendage defect is due to background noise and what percentage is due to an interaction with *tral.* Since three different strengths of *tral* alleles were used in this genetic screen, a deficiency can be concluded to have a true strong interaction with *tral* if the dorsal appendage defect was lowest when crossed with a weak hypomorphic allele, strongest when crossed with a null allele and in the middle when crossed with a strong hypomorphic allele.

Table 2. Sequence Coordinates, Dorsal Appendage Abnormality and Hatching Rate for deficiencies crossed with $tral^{\Delta 4}$.

Genotype	Sequence Coordinates	Number of eggs screened	Number of eggs with Abnormal Appendages	Percentage of Abnormal Appendages	Hatching Rate	Hatching %
Df(3L)ED4515	3L:13,932,272..14,030,132	610	34	5.6%	383/610	62.8%
Df(3L)ED4529	3L:13,932,272..14,070,123	234	21	**9.0%**	138/216	63.9%
Df(3L)ED4528	3L:14,030,141..14,070,123	261	7	2.7%	181/247	73.3%
Df(3L)ED4534	3L:14,030,141..14,186,794	265	49	**18.5%**	204/265	77.0%
Df(3L)ED4978	3L:21,526,907..21,873,785	116	3	2.6%	54/116	46.6%
Df(3L)ED230	3L:22,127,751..22,827,471	116	0	0.0%	38/116	32.8%
Df(3L)ED231	3L:22,864,916..22,938,620	283	9	3.2%	40/41	97.6%
Df(3L)ED4413	3L:8,759,532..8,972,087	200	14	7.0%	135/200	67.5%
Df(3R)ED5156	3R:1,090,655..1,284,574	300	5	1.7%	231/300	77.0%
Df(3R)Exel6144	3R:1,328,532..1,438,438	446	11	2.5%	376/446	84.3%
Df(3R)ED5177	3R:1,426,351..1,449,817	551	31	5.6%	398/551	72.2%
Df(3R)Exel7283	3R:1,474,083..1,572,402	32	0	0.0%	29/32	90.6%
Df(3R)ED5196	3R:1,510,301..1,833,866	319	86	**27.0%**	124/331	37.5%
Df(3R)Exel6145	3R:1,542,490..1,638,975	19	1	5.3%	9/19	47.4%
Df(3R)ED5020	3R:107,408..216,113	17	1	5.9%	5/17	29.4%
Df(3R)ED5092	3R:107,408..912,807	291	0	0%	268/291	92.1%
Df(3R)ED5911	3R:14,568,649..14,991,505	243	12	4.9%	173/243	71.2%
Df(3R)ED5938	3R:14,732,356..15,467,758	368	40	**10.9%**	214/368	58.2%
Df(3R)ED5942	3R:15,052,016..15,660,809	462	24	5.2%	137/259	52.9%
Df(3R)Exel6184	3R:15,289,185..15,467,038	254	13	5.1%	151/254	59.4%
Df(3R)ED6025	3R:15,468,450..16,135,24	200	11	5.5%	140/200	70.0%

Table 2. Sequence Coordinates, Dorsal Appendage Abnormality and Hatching Rate for deficiencies crossed with tral$^{\Delta 4}$(continued).

Df(3R)ED6027	3R:15,662,595..16,135,241	400	11	2.8%	197/400	49.3%
Df(3R)Exel6185	3R:16,135,245..16,376,386	290	9	3.1%	237/290	81.7%
Df(3R)ED6058	3R:17,122,217..17,545,322	239	31	**13.0%**	46/239	19.2%
Df(3R)ED6076	3R:17,459,227..17,868,550	284	10	3.5%	223/284	78.5%
Df(3R)ED6090	3R:17,867,946..18,524,141	259	0	0.0%	155/259	59.8%
Df(3R)ED6096	3R:18,413,403..19,047,691	277	16	5.8%	220/256	85.9%
Df(3R)ED6103	3R:18,724,275..19,084,137	380	80	**21.1%**	200/358	55.9%
Df(3L)ED5017	3R:18,724,275..22,991,401	1054	22	2.1%	775/969	80.0%
Df(3R)ED7665	3R:2,916,249..3,919,805	150	2	1.3%	101/150	67.3%
Df(3R)ED6265	3R:22,937,981..23,405,492	176	5	2.8%	138/176	78.4%
Df(3R)ED6310	3R:24,964,617..25,337,875	238	12	5.0%	72/238	30.3%
Df(3R)Exel6212	3R:25,040,897..25,113,953	241	64	**26.6%**	127/241	52.7%
Df(3R)ED6316	3R:25,081,04..25,608,38	342	29	8.5%	225/342	65.8%
Df(3R)ED5142	3R:279,018..1,090,605	357	7	2.0%	272/357	76.2%
Df(3R)ED5223	3R:3,317,426..3,919,805	809	128	**15.8%**	315/509	61.9%
Df(3R)ED5230	3R:3,803,496..4,478,856	104	0	0.0%	93/104	89.4%
Df(3R)ED5330	3R:4,495,308..5,055,517	393	40	**10.2%**	207/334	62.0%
Df(3R)ED5331	3R:4,859,916..5,055,517	143	12	**8.4%**	84/143	58.7%
Df(3R)ED5095	3R:475,607..912,807	59	2	3.4%	40/59	67.8%
Df(3R)ED5327	3R:5,052,798..5,055,517	359	25	**7.0%**	269/359	74.9%
Df(3R)ED5428	3R:5,456,513..5,874,333	230	1	0.4%	181/230	78.7%
Df(3R)ED5438	3R:5,552,399..5,874,333	231	16	6.9%	155/231	67.1%
Df(3R)ED5454	3R:5,552,399..5,937,180	119	1	0.8%	23/66	34.8%
Df(3R)ED5474	3R:5,935,134..6,176,446	37	2	5.4%	5/22	22.7%
Df(3R)ED5472	3R:5,996,223..6,176,446	119	1	0.8%	23/66	34.8%
Df(3R)ED5506	3R:6,710,720..6,998,470	296	11	3.7%	107/296	36.1%

Table 2. Sequence Coordinates, Dorsal Appendage Abnormality and Hatching Rate for deficiencies crossed with $tral^{\Delta 4}$(continued).

Df(3R)ED5518	3R:6,710,720..7,445,622	246	1	0.4%	180/246	73.2%
Df(3R)ED5138	3R:606,794..1,090,605	226	9	4.0%	99/119	83.2%
Df(3R)ED5516	3R:7,059,89..7,445,622	704	49	7.0%	489/704	68.5%
Df(3R)Exel6143	3R:776,726..912,504	259	39	**15.1%**	179/259	69.1%
Df(3R)ED5610	3R:8,269,738..8,821,397	145	16	**11.0%**	104/145	71.7%
Df(3R)ED5612	3R:8,545,707..9,470,856	223	3	1.3%	167/223	74.9%
Df(3R)ED5613	3R:9,085,471..9,470,856	342	13	3.8%	272/331	82.2%
Df(3R)ED5622	3R:9,509,544..9,809,634	409	20	4.9%	308/409	75.3%
Df(3R)ED5634	3R:9,843,625..10,103,665	284	0	0.0%	236/284	83.1%
Df(3R)ED5147	3R:912,842..1,193,526	486	13	2.7%	470/487	96.5%

From Table 2 detailing the dorsal appendage deficiency and hatching rate for the deficiency crosses with $tral^{\Delta 4}$, it can be concluded that genes located in thirteen different deficiency regions displayed significant interaction with the $tral^{\Delta 4}$ allele. $tral^{\Delta 4}$ is a null mutation and phenotypically, this would be indistinguishable from a deletion of *tral*; as a result, it would be expected that a strong dorsal appendage defect should signify a positive interaction with *tral.* The deficiencies that displayed a strong interaction when crossed with the $tral^{\Delta 4}$ allele included Df(3L)ED4529, Df(3L)ED4534, Df(3R)ED5196, Df(3R)ED5938, Df(3R)ED6103, Df(3R)Exel6212, Df(3R)ED5223, Df(3R)ED5330, Df (3R)ED5331, Df(3R)ED6058, Df(3R)Exel6143, and Df(3R)ED5610. Although other deficiencies also produced eggs with ventralized dorsal appendages, the percentage of eggs that exhibited abnormal appendages was too low to indicate a strong interaction and therefore they were not analyzed further. The cutoff for a strong interaction was 8.0% and greater to ensure that the interaction seen from the dorsal appendage defect was not background noise but a real interaction. When the deficiencies were crossed with $tral^{KG08052}$, if there was an interaction between the deficiencies and this weak hypomorphormic allele, the percentage of eggs with deformed dorsal appendages was minimal. When the deficiencies were crossed with $tral^{e03082}$, a strong hypomorphic allele, the interactions for most of the deficiencies was around 5%. Therefore, in order for the interaction with $tral^{\Delta 4}$ to be considered great, a cutoff point that was higher than this percentage was chosen to ensure that the dorsal appendage accounted for was a result of an interaction between the deficiency stock and *tral.*

Table 3. Sequence Coordinates, Dorsal Appendage Abnormality and Hatching Rate for deficiencies crossed with $tral^{e03082}$.

Genotype	Sequence Coordinates	Number of eggs screened	Number of eggs with Abnormal Appendages	% of Abnormal Appendages	Hatching Rate	Hatching %
Df(3L)ED4515	3L:13,932,272..14,030,132	257	0	0.0%	14/104	13.5 %
Df(3L)ED4529	3L:13,932,272..14,070,123	334	19	5.7%	225/334	67.4 %
Df(3L)ED4528	3L:14,030,141..14,070,123	594	9	1.5%	143/230	62.2 %
Df(3L)ED4534	3L:14,030,141..14,186,794	211	6	2.8%	140/211	66.4 %
Df(3L)ED4978	3L:21,526,907..21,873,785	395	14	3.5%	281/395	71.1 %
Df(3L)ED230	3L:22,127,751..22,827,471	80	3	3.8%	11/80	13.8 %
Df(3L)ED231	3L:22,864,916..22,938,620	252	3	1.2%	193/261	74.0 %
Df(3L)ED4413	3L:8,759,532..8,972,087	257	12	4.7%	130/255	51.0 %
Df(3R)ED5156	3R:1,090,655..1,284,574	787	57	7.2%	221/253	87.4 %
Df(3R)Exel6144	3R:1,328,532..1,438,438	276	8	2.9%	125/249	50.2 %
Df(3R)ED5177	3R:1,426,351..1,449,817	363	3	0.8%	310/363	85.4 %
Df(3R)Exel7283	3R:1,474,083..1,572,402	209	8	3.8%	103/209	49.3 %
Df(3R)ED5197	3R:1,474,504..1,833,866	223	28	**12.6%**	97/223	43.5 %
Df(3R)ED5196	3R:1,510,301..1,833,866	585	28	4.8%	421/585	72.0 %
Df(3R)Exel6145	3R:1,542,490..1,638,975	73	3	4.1%	37/73	50.7 %
Df(3R)ED5020	3R:107,408..216,113	276	13	4.7%	174/276	63.0 %
Df(3R)ED5092	3R:107,408..912,807	255	15	5.9%	145/255	56.9 %
Df(3R)ED5911	3R:14,568,649..14,991,505	76	0	0.0%	25/76	32.9 %
Df(3R)ED5938	3R:14,732,356..15,467,758	292	14	4.8%	199/292	68.2 %
Df(3R)ED5942	3R:15,052,016..15,660,809	210	20	**9.5%**	278/380	73.2 %
Df(3R)Exel6184	3R:15,289,185..15,467,038	191	9	4.7%	105/191	55.0 %

Table 3. Sequence Coordinates, Dorsal Appendage Abnormality and Hatching Rate for deficiencies crossed with tral^{e03082} (continued).

Df(3R)ED6025	3R:15,468,450..16,135,24	280	20	7.1%	111/280	39.6%
Df(3R)ED6027	3R:15,662,595..16,135,241	363	40	**11.0%**	266/363	73.3%
Df(3R)Exel6185	3R:16,135,245..16,376,386	17	7	**41.2%**	12/17	70.6%
Df(3R)ED6058	3R:17,122,217..17,545,322	207	5	2.4%	164/207	79.2%
Df(3R)ED6076	3R:17,459,227..17,868,550	1590	75	4.7%	896/1590	56.4%
Df(3R)ED6090	3R:17,867,946..18,524,141	247	0	0.0%	156/247	63.2%
Df(3R)ED6091	3R:18,413,403..18,552,029	585	17	2.9%	496/585	84.8%
Df(3R)ED6096	3R:18,413,403..19,047,691	315	8	2.5%	202/315	64.1%
Df(3R)ED6103	3R:18,724,275..19,084,137	142	6	4.2%	130/142	91.5%
Df(3L)ED5017	3R:18,724,275..22,991,401	534	32	6.0%	267/373	71.6%
Df(3R)ED7665	3R:2,916,249..3,919,805	42	0	0.0%	25/42	59.5%
Df(3R)ED6232	3R:21,862,598..22,624,704	227	1	0.4%	163/227	71.8%
Df(3R)ED6265	3R:22,937,981..23,405,492	102	9	**8.8%**	90/102	88.2%
Df(3R)ED6242	3R:22,966,066..23,089,591	139	14	**10.1%**	109/139	78.4%
Df(3R)ED6310	3R:24,964,617..25,337,875	147	0	0.0%	85/147	57.8%
Df(3R)Exel6212	3R:25,040,897..25,113,953	208	19	**9.1%**	143/208	68.8%
Df(3R)ED6316	3R:25,081,04..25,608,38	390	25	6.4%	292/390	74.9%
Df(3R)ED5142	3R:279,018..1,090,605	632	32	5.1%	444/632	70.3%
Df(3R)ED5223	3R:3,317,426..3,919,805	513	7	1.4%	394/513	76.8%
Df(3R)ED5230	3R:3,803,496..4,478,856	210	6	2.9%	160/210	76.2%
Df(3R)ED5331	3R:4,859,916..5,055,517	259	23	8.9%	128/259	64.9%
Df(3R)ED5095	3R:475,607..912,807	93	1	1.1%	90/93	96.8%
Df(3R)ED5327	3R:5,052,798..5,055,517	198	2	1.0%	175/198	88.4%
Df(3R)ED5428	3R:5,456,513..5,874,333	317	2	0.6%	202/279	72.4%
Df(3R)ED5438	3R:5,552,399..5,874,333	498	12	2.4%	221/498	44.4%
Df(3R)ED5454	3R:5,552,399..5,937,180	200	0	0.0%	68/200	34.0%
Df(3R)ED6025	3R:15,468,450..16,135,24	280	20	7.1%	111/280	39.6%

Table 3. Sequence Coordinates, Dorsal Appendage Abnormality and Hatching Rate for deficiencies crossed with tral^{e03082} (continued).

Df(3R)ED5474	3R:5,935,134..6,176,446	288	6	2.1%	238/288	82.6%
Df(3R)ED5472	3R:5,996,223..6,176,446	200	0	0.0%	68/200	34.0%
Df(3R)ED5506	3R:6,710,720..6,998,470	237	8	3.4%	87/131	66.4%
Df(3R)ED5518	3R:6,710,720..7,445,622	394	0	0.0%	159/394	40.4%
Df(3R)ED5138	3R:606,794..1,090,605	200	11	5.5%	191/200	95.5%
Df(3R)ED5516	3R:7,059,89..7,445,622	208	14	6.7%	129/208	62.0%
Df(3R)ED5591	3R:8,176,253..8,545,732	193	20	**10.4%**	90/193	46.6%
Df(3R)ED5610	3R:8,269,738..8,821,397	192	8	4.2%	115/192	59.9%
Df(3R)ED5613	3R:9,085,471..9,470,856	280	0	0.0%	202/280	72.1%
Df(3R)ED5622	3R:9,509,544..9,809,634	407	28	6.9%	207/361	57.3%
Df(3R)ED5634	3R:9,843,625..10,103,665	142	3	2.1%	69/142	48.6%
Df(3R)ED5644	3R:9,843,625..10,451,431	190	10	5.3%	125/190	65.8%
Df(3R)ED5147	3R:912,842..1,193,526	280	29	**10.4%**	154/280	55.0%

tral^{e03082} is a PiggyBAC transposon insertion in the 5' UTR of *tral* and has been shown to be a strong hypomorphic mutation since ninety-three percent of eggs laid by *tral*^{KG08052}/*tral* ^{e03082} females displayed ventralized eggshells (Wilhelm et al., 2005). As a result, it is expected that of the three different alleles of *tral* tested for this genetic screen, the ventralized eggshell defect would be intermediate for deficiency stocks crossed with *tral*^{e03082}. From the data presented regarding the dorsal appendage abnormality and hatching rates of the crosses (Table 3), it can be concluded that genes from certain deficiencies had a significant effect on the dorsal appendage formation when crossed with this allele of *tral.* The deficiencies that displayed a significant effect in ventralized eggshell formation included Df(3R)ED5197, Df(3R)ED5942, Df(3R)ED6027, Df(3R)Exel6185, Df(3R)ED6265, Df(3R)ED6242, Df(3R)Exel6212, Df (3R)ED5591 and Df(3R)ED5147.

The data presented concerning the deficiency crosses with the three different alleles of *tral* (Table 1, Table 2 and Table 3) can be combined further to determine regions on chromosome three that produced a genetic interaction with *tral*. The deficiencies that were considered to have a strong interaction were further analyzed and narrowed down to pinpoint genes located within the deficiency region that genetically interact with *tral.* To do so, any deficiencies that resulted in high dorsal appendage defects when crossed with tral$^{\Delta 4}$ and had moderate defects when crossed with tral^{e03082} were further subdivided into smaller regions to be crossed again with the three alleles of *tral* in order to narrow the region on the third chromosome from which the genes would be located. In the genetic screen of the deficiency stocks, those that

produced strong dorsal appendage defects when crossed with $tral^{\Delta 4}$ or with $tral^{e03082}$ included Df(3R)ED5196, Df(3R)ED5223, Df(3R)ED5331, Df(3R)ED5327, Df(3R)ED6316, Df(3R)ED5942, Df(3R)ED6265, Df(3R)ED6103, Df(3R)ED5156, Df(3R)ED5330, Df(3L)ED4534, Df(3L)ED4529, Df(3L)ED4413 and Df(3R)ED5610 (Table 4).

Table 4. Genotype, Sequence Coordinates, Dorsal Appendage Abnormality for deficiencies that display strong overall dorsal appendage defects.

Genotype	Sequence Coordinates	Abnormal Appendages in *tral*^{KG08052}	Abnormal Appendages in *tral*$^{\Delta 4}$	Abnormal Appendages in *tral*^{e03082}
Df(3L)ED4529	3L:13,932,272..14,070,123	0.90%	9.00%	5.70%
Df(3L)ED4534	3L:14,030,141..14,186,794	0.00%	18.50%	2.80%
Df(3L)ED4413	3L:8,759,532..8,972,087	0.60%	7.00%	4.70%
Df(3R)ED5156	3R:1,090,655..1,284,574	0.00%	1.70%	7.20%
Df(3R)ED5196	3R:1,510,301..1,833,866	4.80%	27.00%	4.80%
Df(3R)ED5942	3R:15,052,016..15,660,809	3.70%	5.20%	9.50%
Df(3R)ED6025	3R:15,468,450..16,135,241	0.70%	5.50%	7.10%
Df(3R)ED6103	3R:18,724,275..19,084,137	0.70%	21.10%	4.20%
Df(3R)ED6265	3R:22,937,981..23,405,492	0.90%	2.80%	8.80%
Df(3R)ED6316	3R:25,081,045..25,608,389	3.80%	8.50%	6.40%
Df(3R)ED5223	3R:3,317,426..3,919,805	1.80%	15.80%	1.40%
Df(3R)ED5330	3R:4,495,308..5,055,517	1.90%	10.20%	
Df(3R)ED5331	3R:4,859,916..5,055,517	2.90%	8.40%	8.90%
Df(3R)ED5327	3R:5,052,798..5,055,517	3.90%	7.00%	1.00%
Df(3R)ED5610	3R:8,269,738..8,821,397	0.50%	11.00%	4.20%

The boundaries of the deficiencies generated by the Bloomington Fly Stock Center were mapped using the GBrowse function on Flybase (www.flybase.org). Deficiencies that contained overlapping regions were classified together in order to see which regions on the third chromosome interacted with *tral.* If two overlapping deficiencies both produced strong dorsal appendage defects, then it was concluded that the region shared between the two deficiencies was important for the genetic interaction with *tral.* The regions of interest were analyzed to see if it was possible to identify specific genes within each region that were responsible for the interaction. At the end of this chapter are the figures and tables that show the regions in the third chromosome that contained the candidate genes (Figures 4-15 and Tables 5-13). But, first, the four genes of interest that were thought to genetically interact with *tral* will be discussed.

string

In the span of 3R:25,081,045..25,618,389, the one candidate gene that was thought to interact with *tral* was *string,* a protein tyrosine phophatase that has a role in regulation of the mitotic cell cycle. The dorsal appendage defect when the deficiency stock was crossed with the three alleles of *tral* was 3.80% when crossed with $tral^{KG08052}$, 8.50% when crosses with $tral^{A4}$ and 6.40% when crossed with $tral^{e03082}$.

Stg is necessary and sufficient to trigger mitosis after the formation of the cellular blastoderm (Reed, 1995). Mitosis before interphase 14 runs on maternal products but after interphase 14 requires zygotic transcription products and occurs in a spatio-temporal pattern. Mutations of *stg* cause cell-cycle arrest but do not arrest other aspects of development, implying that *stg* is required specifically for initiating mitosis (O'Farrell et al., 1989). The activator of mitosis encoded by the *stg* gene is a positive regulator of cdc2 kinase (cdk2), which is associated with other proteins that are required to regulate its mitosis-promoting activity. Cdk2 acts with cyclin E to control transition from G phase to S phase during mitosis. Following mitosis 13, maternally provided mRNAs, including *stg,* are degraded and the cell cycle of the embryo is no longer synchronous. Because *stg* is believed to be unstable and short-lived, its transcription is rate-limiting for cell division (Reed, 1995).

Embryos lacking *stg* undergo no mitotic divisions after M13 and arrest at the G2/M boundary of the fourteenth division cycle. These embryos will still gastrulate and develop substantially. This phenotype suggests that many aspects of development

have no requirement for a critical number of cells or for passage through a certain number of cell cycles (Reed, 1995).

Since *stg* transcription controls the mitosis in the postblastoderm embryo, there may be a relationship between the pattern formation genes and the transcriptional regulation of *stg.* Mutations in pattern formation genes also show changes in the patterns of mitosis; however, there is not a simple relationship between the expression pattern of *stg* with that of pattern formation genes. It can therefore be concluded that regulated expression of *stg* mRNA controls the timing and location of these embryonic cell divisions (Reed, 1995).

It can be hypothesized that *stg* disrupts the activation of Cdk2, disrupting the mitotic cell cycle. Flies homozygous for a *cycE* mutant lay eggs with thin and fragile outer eggshells, suggesting that a defect in the chorion gene amplification occurs during the follicle cell endoreplication. Since Cdk2 and CycE act together, when one or both components of this regulatory pathway are disrupted, dorsoventral patterning will also be altered. As a result, it is perceived that faulty DNA replication in nurse cells can alter *grk* regulation since disruption of the mitotic cycle leads to reduced transcription. The fact that the mitotic checkpoint leads to cell cycle arrest then provides a theory for how localized expression of *grk* is affected and how this gene may possibly interact with *tral* (MacDonald et al., 2007).

To ensure that *stg* was the gene responsible for the genetic interaction with *tral*, a null mutation deficiency stock of *stg* was obtained from the Bloomington Stock Center at Indiana University. This null mutation stock was then crossed with the three

different alleles of *tral* described above. From these crosses, 2.3% of the eggs produced from the cross with $tral^{KG08052}$, 0.91% of the eggs produced from the cross with $tral^{\Delta 4}$, and 1.6% of the eggs produced from the cross with $tral^{e03082}$ displayed fused or no dorsal appendages. If there was a true genetic interaction between *stg* and *tral*, then the expected dorsal appendage defect would be similar to the cross of the null mutation and the original deficiency stock lacking *stg.* However, as seen in the percentages of eggs counted that had defective dorsal appendage formation, there was little effect of the *stg/tral* double heterozygous mutant. As a result, further experiments were not conducted on *stg* to determine if there was genetic interaction with *tral.* It can be concluded that either the original dorsal appendage defect was a false positive or that mutations in mitotic cell cycle checkpoint genes such as *stg* may interrupt *grk* expression on their own, which causes an abnormality in the dorsal appendage formation. An explanation for why the deficiency in this region interacted is that there is an undocumented gene in this region that is responsible for the interaction with *tral.* Another explanation is that they may be mobile elements, such as small interfereing RNA (siRNA), that is moved around when the introns are spliced out, since it will interfere with the expression of the gene. Another possibility is that when *stg* was deleted, it could have also taken out a promoter enhancer that could have been responsible for other components involved in the secretion pathway. This would then explain the interaction with *tral* first noted when the deficiency stock was crossed with the three aleles of *tral.*

CG16718

There are no genes that completely overlap among the deficiencies in the region 3R:15082016..15638909; however, the two deficiencies that have strong interactions with *tral* both result in a breakpoint in the gene CG16718, a member of the Aberrant X segregation (Axs) transmemberane protein family. Axs protein localizes to the ER in early *Drosophila* embryos and a membranous sheath-like structure associates with the meiotic spindle in oocytes. Mutations in the Axs genes therefore disrupt chromosome segregation and meiotic spindle assembly (Hawley et al., 2003).

The *Saccharomyces serecisiae* ortholog, *Ist2p,* is a plasma membrane protein. *Ist2p* mRNA localization leads to the accumulation of the protein at the plasma membrane of the daughter cells. In addition, trafficking of Ist2p is independent of myosin mediated vesicular transport, a characteristic of the standard secretory pathway which implies that trafficking of Ist2p does not require classical secretory machinery and that a novel trafficking pathway might be connecting specialized domains of the ER with the plasma membrane (Seedorf et al., 2004). Therefore, we wanted to see if this was conserved in *Drosophila* since it suggests a possible link between the mRNA localization and membrane trafficking functions of *tral.* In order to test this possibility, we performed *in situ* hybridization experiments to determine CG16718's mRNA localization in the *Drosophila* oocyte and if the mRNA or protein-localization was *tral*-dependent..

Oocyte maturation involves the meiotic cell cycle and changes in the oocyte cytoplasm. More specifically, restructuring occurs in the ER and changes in calcium physiology occur (Hawley et al., 2003). CG16718 is thought to be a homolog of ANO1, an activated chloride channel that mediates receptor activated chloride currents (Oh et al., 2008). Since CG16718 is thought to be an Axs-like protein, it encloses the female meiotic spindle and mutations in this gene will cause defects in spindle assembly and chromosome segregation. Microtubules are also required for the transport of mRNAs to the oocyte in order for polarity to be established in oocytes (Macdonald et al., 2007). It is known that CG16718 mRNA is localized as in yeast and that *tral* plays a role in its localization. Therefore, if CG16718 is localized similarly in *Drosophila,* then it can be concluded that CG16718 is a candidate mRNA target of *tral.*

Through *in situ* experiments (Figure 2), oocytes were analyzed to determine where the mRNA localizes in the Df(3R)ED6025/Df(3R)ED5938 mutant. These mutants were heterozygous for the two deficiency stocks that had breakpoints in the CG16718 gene. *In situ* hybridization using the antisense strand of Df(3R)ED6025/Df(3R)ED5938 revealed noticeable staining of the outer follicle cells (Figure 2A). The same expression can be seen in the sense probe of the same mutants (Figure 2B). Because the sense strand *in situ* experiment is not supposed to produce any expression, figure 2A and 2B indicate that the expression detected using the antisense CG16718 probe in Df(3R)ED6025/Df(3R)ED5938 *in situ* was background noise. In addition, the staining in the Df(3R)ED6025/Df(3R)ED5938 double mutant

does not seem to vary in expression when compaed to CG16718 sense and antisense probe *in situ* experiments in ORER controls (Figure 2C and Figure 2D). This can be attributed to the fact that the mRNA is too low to be detected by *in situ*. Because the antisense *osk* control is localized posteriorly in the oocyte, we know that the *in situ* technique worked properly and that the CG16718 *in situ* experiment probably did not work due to faulty CG16718 probes created. As a result, further experiments need to be done to confirm any possible interaction with *tral* and CG16718 with a focus on determining the level of CG16718 expression in the ovary.

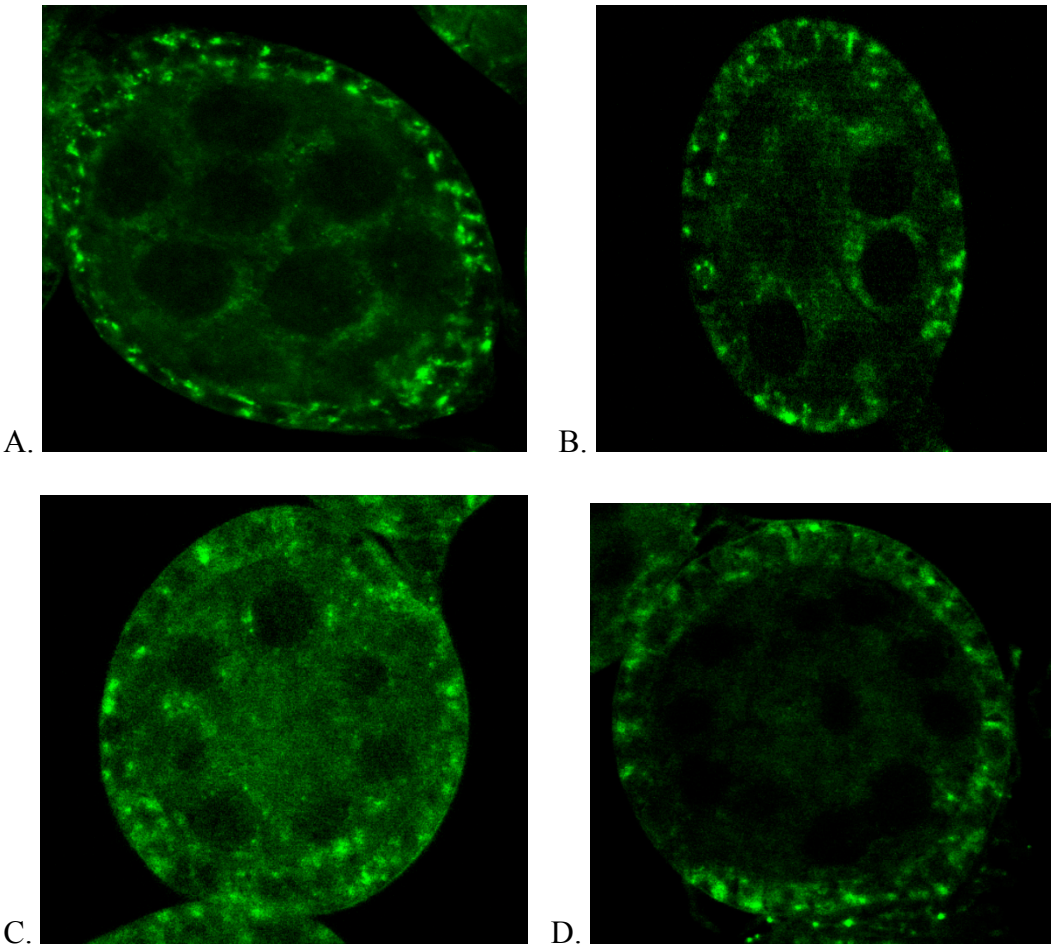

Figure 2. In situ expression patterns of CG16718. (A) 500 bp antisense probe shows staining in the outer follicle cells in Df(3R)ED6025/Df(3R)ED5938 oocytes at stage E5. (B) Sense negative control probe also shows the staining of the outer follicle cells in Df(3R)ED6025/Df(3R)ED5938 oocytes in early stage 5. (C) 500 bp antisense probe serving as a control for staining in ORER oocytes. (D) Sense negative control probe in ORER oocytes.

cap 'n' collar

In the span of 3R:18947691..19147690, possible gene candidates were narrowed down to twelve genes; however, because of the biological processes including oocyte dorsal/ventral axis specification associated with the gene *cap 'n' collar (cnc)*, further experiments were conducted to determine its interaction with *tral*.

Cnc is a basic-leucine zipper homeotic gene that functions with a homeotic gene *Deformed (Dfd)* to specify mandibular development (Mohler et al., 1995). It plays a role in cephalic patterning during *Drosophila* embryogenesis (Mohler et al., 1991). Mandibular and labral structures are missing in *cnc* mutant larvae due to a failure to maintain the patterns of labral-specific segment polarity (Mohler et al., 1995).

In *Drosophila,* dorsal-ventral polarity is established by the asymmetric positioning of the oocyte nucleus. Normally, the oocyte nucleus migrates from a posterior position to an anterior-dorsal position. However, in *cnc* mutants, the oocyte nucleus correctly migrates until stage 9 of oogenesis. At the end of stage 9, the nucleus moves from the anterior pole towards the posterior pole. In addition to the mislocalization of the oocyte nucleus, there is failure to maintain *bcd* mRNA at the anterior pole and *osk* mRNA at the posterior pole. *grk* mRNA still associates with the oocyte nucleus in *cnc* mutants and the secretion of the Grk protein is still able to activate the *Drosophila* EGF receptor in the dorsal follicle cells; however even with the presence of proper Grk signaling during stage 9, *cnc* mutants still lack dorsoventral

polarity, thereby allowing for the study of the influence of Grk signaling on dorsoventral patterning in the follicular epithelium (Roth et al., 2001).

In addition to the migration of the mRNAs to the correct poles, it is also important for the nucleus at the anterior cortex of the oocyte to be anchored for proper dorsal-ventral axis formation to occur. In *cnc* mutants, nuclear migration occurs normally in the earlier stages. But, later in oogenesis, the nucleus slides back towards the posterior pole rather than remain at the anterior cortex. The mislocated nucleus is tightly associated with the actin network, implying that it remains attached to the plasma membrane of the oocyte. In *cnc* mutants, the nucleus is randomly positioned within the oocyte and *grk* transcripts remain associated with the misplaced nucleus, implying that *cnc* plays a role in the anchoring of the nucleus to the anterior cortex of the oocyte and that the failure to anchor the nucleus is responsible for both the mislocalized *grk* mRNA and the disruption of dorsal-ventral patterning (Roth et al., 2001). In order to test this hypothesis, $tral^{ED4483}$/*cnc* mutant oocytes were stained using immunofluorescence to determine where the Cnc protein is localized (Figure 3).

From previous experiments performed by Roth et al., 2001, it was known that *cnc* mutant affects the localization of the oocyte nucleus. Germline clones were made and the mutant egg chambers were screened to determine the defects in the lozalization of both *osk* and *grk* mRNAs. Since germ line clones were made, it is known that the cnc function is in the germ line and not the follicle cells. Usually, Cnc protein is found in both germline and somatic nuclei, but greater amounts of the

protein are found in the germline. In addition, Cnc protein is present at all stages during oogenesis and in the oocyte nucleus at stage 9 (Roth et al., 2001).

From the immunofluorescence imaging (Figure 3), it is clear that some Cnc protein accumulates in the nurse cells during stage 8 of the yw ovaries. Because *grk* transcripts remain associated with the misplaced nucleus and the oocyte nucleus is mislocalized in egg chambers lacking *cnc*, it was hypothesized that the Cnc protein would be distributed differently in *cnc/tral* mutants from yw ovaries. However, the staining for the mutants and control showed the protein expression to be about equal. Therefore, more experiments have to be conducted spanning more stages of oogenesis in order to fully understand the molecular basis for how *cnc* genetically interacts with *tral.*

Because *grk* mRNA is correctly localized through stage 9 in *cnc* mutants, one possible explanation for the ventralization of the eggshell is that *cnc* is required for translational regulation of *grk* mRNA (Roth et, al, 2001). Immunofluorescence studies revealed that Grk protein expression and localization was similar between the yw control and the *cnc/tral* mutants, which would imply that the ventralization is not due to lack of *grk* transcription or translation.

Drosophila eggshell patterning is dependent on integration of Grk signaling with Decapentalplegic (Dpp), a TGF-ß member that appears to enhance the levels of the EGF pathway though signaling from anterior follicle cells. Even through correct Grk signaling was detected up to stage 9 in oogenesis, the signal was not strong enough to initiate the required Dpp signaling to ensure correct dorsal-ventral

patterning, providing an explanation for *cnc* interaction with *tral*. Because *cnc* mutants cannot maintain anterior anchoring of the oocyte nucleus, it is most likely not possible for *cnc* egg chambers to form a zone where Grk and Dpp signaling inputs can overlap to allow for correct anterior-dorsal follicle patterning. Since anterior-dorsal follicle pattering is not established correctly, dorsal appendage formation will also not proceed correctly (Roth et al, 2001).

Since Cnc is a transcription factor, it can be concluded that it is responsible for the control of expression of proteins needed to establish the components of the anterior anchor. Disruption of this gene and protein will result in lack of dorsoventral polarity. Even though Grk is secreted to activated EGF receptors in the dorsal follicle cells, the signal is too weak to induce proper stable dorsoventral follicle cell patterning since the oocyte nucleus migrates before stage 10A, which is the stage that EGF receptor activation by Grk must be maintained until for the establishment of the correct dorsal-ventral polarity axis (Roth et al., 2001).

A. 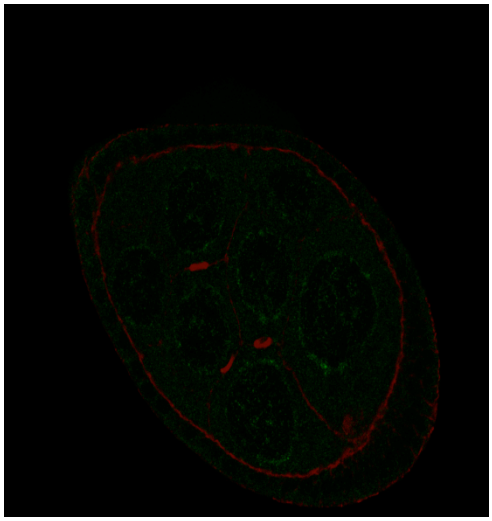 B. 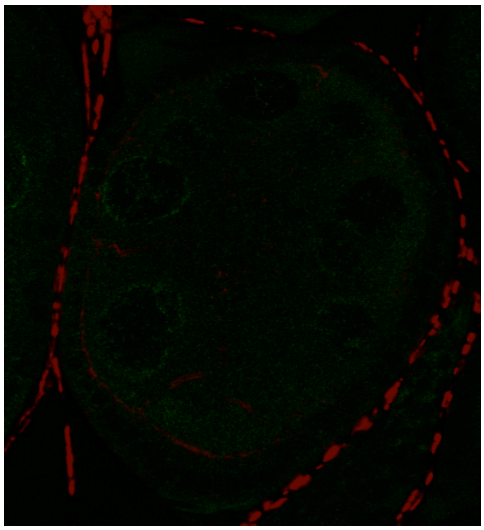

Figure 3. *Cap 'n' collar* antibody staining expression patterns. (A-B) Double labeling for Cnc protein (green) and actin (red) in ED4483/tral^{KG08052} and yw embryos. (A) Cap 'n" collar antibody staining for ovaries of tral^{ED4483}/cnc mutants during stage 8 (B) *cap 'n' collar* staining of yw ovaries at stage 8.

pumilio

In the span of 3R:4,858,916..5,065,517, the overlapping regions of three deficiencies indicated that pum, a gene that controls germline stem cells in *Drosophila* females, was a possible candidate for interaction with *tral* (Kimble et. al, 2002).

Pum works with a zinc-finger protein Nanos to repress the translation of maternal *hunchback* RNA in the posterior of the *Drosophila* embryo to allow for abdomen formation (Lehmannn et al., 1998). *Nanos* RNA is localized to the posterior pole during oogenesis and the posteriorly synthesized Nanos protein is sequestered into the germ cells as the embryo is formed. Maternally deposited Nanos protein must also be present for germ cell migration. During oogenesis, *nanos* and *pumilio* both affect the germline stem cell development but only *pumilio* mutant ovaries fail to maintain stem cells and therefore all germline cells differentiate into egg chambers. Pum contains a RNA-binding domain and binds to *nanos* response elements. Even though it is ubiquitously distributed in the embryo, it is only active in the repression of the *hb* translation in the posterior area, which indicates that the interaction between Pum and posteriorly localized Nanos will mediate translational repression (Murata and Wharton, 1995).

Axial patterning of the *Drosophila* oocyte relies on the position of certain mRNAs and proteins at specific locations within the developing oocyte (Macdonald et. al., 2007). In order for patterning to occur correctly, transport of the mRNAs from the nurse cells to the oocyte, localization of the mRNAs to the correct location and time must occur within the oocyte and translational regulation of the mRNA must be

done to ensure proper distribution of the proteins to the correct area. *pum* is a gene that acts as the translational regulator to ensure that embryonic patterning and germline development occur properly. *pum* is required for stem cell regulation and embryonic patterning, but it has been shown to have a dorsal ventral patterning defect in the oocyte. This may be due to the nature of the alleles that have been used in previous work. Our studies suggest an additional role for *pum* in *grk* regulation. Further studies directed at identificying the role of *pum* in mid oogenesis will likely uncover a novel role for *pum* mediated translational control in Grk signaling and dorsal ventral pattern formation.

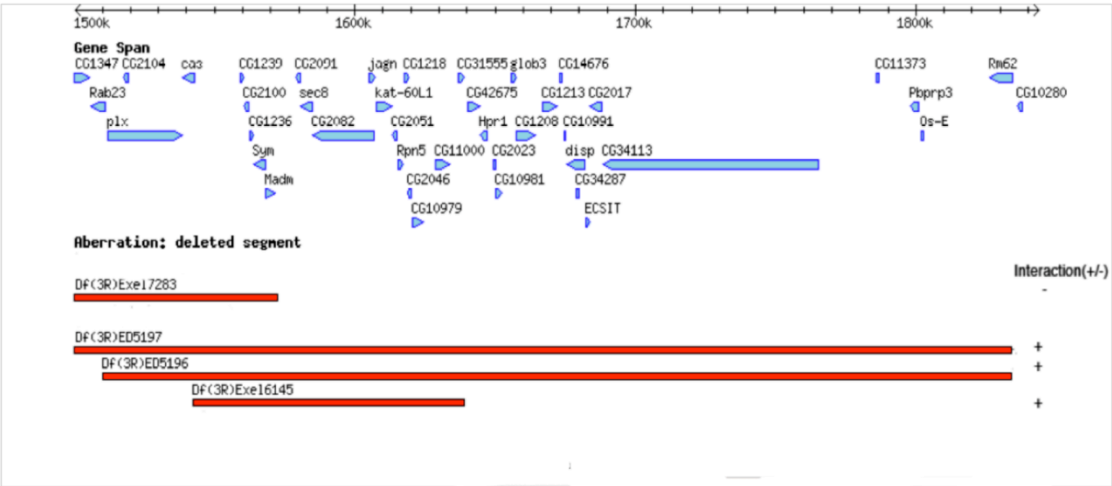

Figure 4. Gene span showing the genes and regions for the deficiency stocks for 3R:1,500,301..1,843,866. By analyzing the regions that resulted in dorsal appendage deects when crossed with the three alleles of *tral,* possible candidate genes could be identified.

Table 5. Possible genes that may interact with *tral* on chromosome three within the span of 3R:1,500,301..1,843,866.

Gene	Biochemical Function/Homolog
CG10979	Zinc ion Binding Function
CG11000	Unknown
CG1218	Unknown
CG2046	Unknown
CG2051	Histone acetyltransferase activity, histone acetylation, chromatin silencing at telomere
CG2082	Unknown
CG2091	Protein binding. Hydrolase activity, deadenylation-dependent decapping of nuclear-transcribed mRNA
CG31555	Unknown
Jagn	Vitellogenesis, bristle development, oocyte growth, establishment of ER localization, exocytosis, endoplasmic reticulum organization, bristle morphogenesis
Kat-60L1	ATPase activity, microtubule binding, neuron remodeling
Rpn5	Endopeptidase activity; proteolysis
Sec8	Regulation of synapse structure and activity

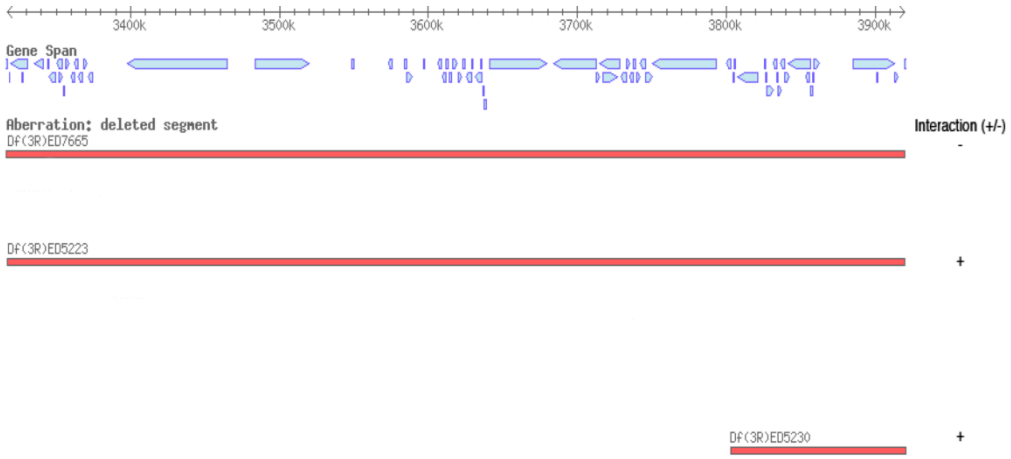

Figure 5. Gene span showing the genes and regions for the deficiency stocks for 3R:3,317,226..3,919,905. By analyzing the regions that resulted in dorsal appendage deects when crossed with the three alleles of *tral,* possible candidate genes could be identified.

Table 6. Possible genes that may interact with *tral* on chromosome three within the span of 3R:3317226..3919905.

Gene	Biochemical Function/Homolog
CG10903	S-adenosylmethionine-dependent methyltransferase activity; metabolic process
CG11035	Chaperone binding
CG11052	Acylphosphatase activity
CG10435	Unknown
CG14463	Unknown
CG2698	Unknown
CG2747	Binding Function
CG2767	Alcohol dehydrogenase activity
CG2781	Fatty acid elongase activity
CG3223	Unknown
CG42550	Unknown
CG7910	Fatty acid amide hydrolase activity
CG7918	Muscarinic acetyloine receptor activity
ImpE3	Imaginal disc eversion
Os-C	Phermone binding
Pbp95	DNA binding; protein binding
Sfp84E	Unknown
snoRNA:Me18S-G432	Unknown
Tom34	Binding Function

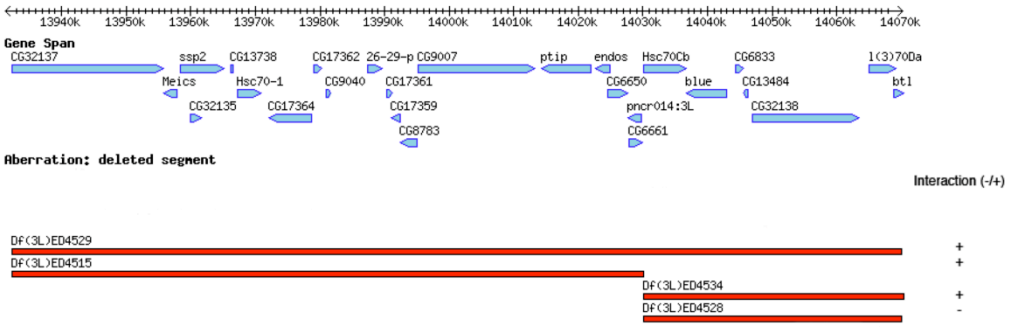

Figure 6. Within the region 3L:13,931,272..14,070,223, it was narrowed down to gene Hsc70Cb, a gene with biological processes of chaperone binding and protein binding as a candidate responsible for the strong dosal-ventral defect.

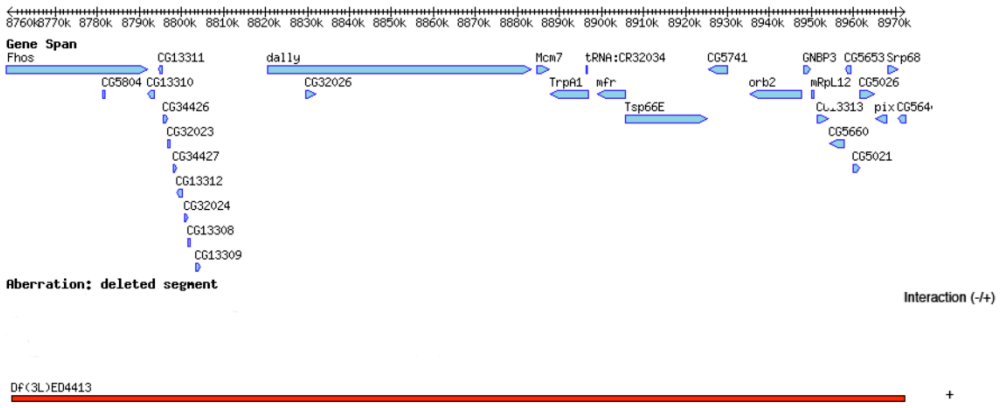

Figure 7. Gene span showing the genes and regions for the deficiency stocks for 3L:8,758,532..8,972,187. By analyzing the regions that resulted in dorsal appendage deects when crossed with the three alleles of *tral,* possible candidate genes could be identified.

Table 7. Possible genes that may interact with *tral* on chromosome three within the span of 3L:8,758,532..8,972,187.

Gene	Biochemical Function/Homolog
CG13308	Actin binding
CG13309	Cellular acyl-CoA homeostasis
CG13310	Unknown
CG13311	Metabolic Processes
CG13312	Chitin Binding
CG13313	Unknown
CG32023	Unknown
CG32024	Chitin Binding
CG32026	Isocitrate dehydrogenase activity
CG32033	Unknown
CG34426	Unknown
CG34427	Unknown
CG5021	Unknown
CG5026	Dephosphorylation
CG5644	Unknown
CG5653	Unknown
CG5660	Valyl-tRNA aminoacylation
CG5741	Unknown
CG5804	Diazepam binding, enzyme inhibitor activity, acyl-coA binding
dally	Protein binding
Fhos	Actin binding
GNBP3	Pattern recognition receptor activity
Mcm7	3'-5' DNA helicase activity
mfr	Chorion-containing eggshell pattern formation
mRpL12	Chromatin binding
Orb2	mRNA binding
Pix	Ribosomal small subunit binding, ATP binding
Srp68	7S RNA binding, mRNA binding
tRNA:CR32034	Unknown
TrpA1	Calcium channel activity
Tsp66E	Unknown

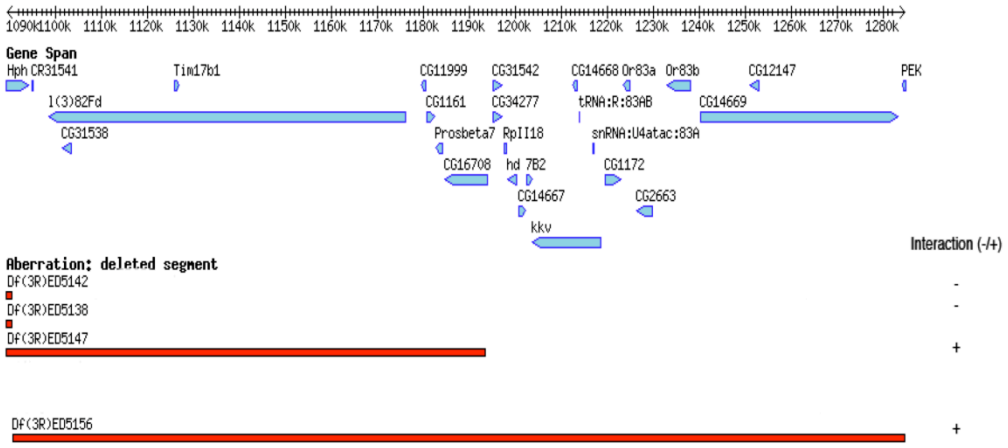

Figure 8. Gene span showing the genes and regions for the deficiency stocks for 3R:1,089,555..1,284,674. By analyzing the regions that resulted in dorsal appendage deects when crossed with the three alleles of *tral,* possible candidate genes could be identified.

Table 8. Possible genes that may interact with *tral* on chromosome three within the span of 3R:1,089,555..1,284,674.

Gene	Biochemical Function/Homolog
CG1161	Unknown
CG31538	Unknown
CR31541	Unknown
l(3)82Fd	Unknown
Prosbetta7	Endopeptidase activity
Tim17b1	Protein targeting to mitochondrion, protein transport

Figure 9. Within the region 3R:4,858,916..5,065,517, it was narrowed down to *pumilio*, a gene that controls germline stem cell, as a candidate responsible for the strong dorsal-ventral defect.

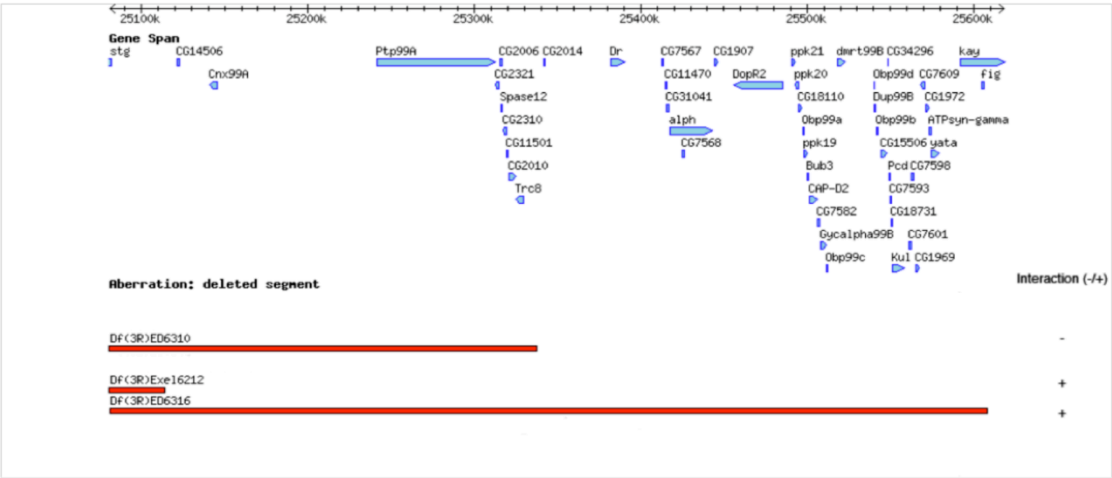

Figure 10. Within the region 3R:4,858,916..5,065,517, it was narrowed down to 3R:25,081,045..25,618,389, it was narrowed down to *string*, a protein tyrosine phosphatase that has a role in regulaion of the mitotic cell cycle, as a candidate responsible for the strong dorsal-ventral defect.

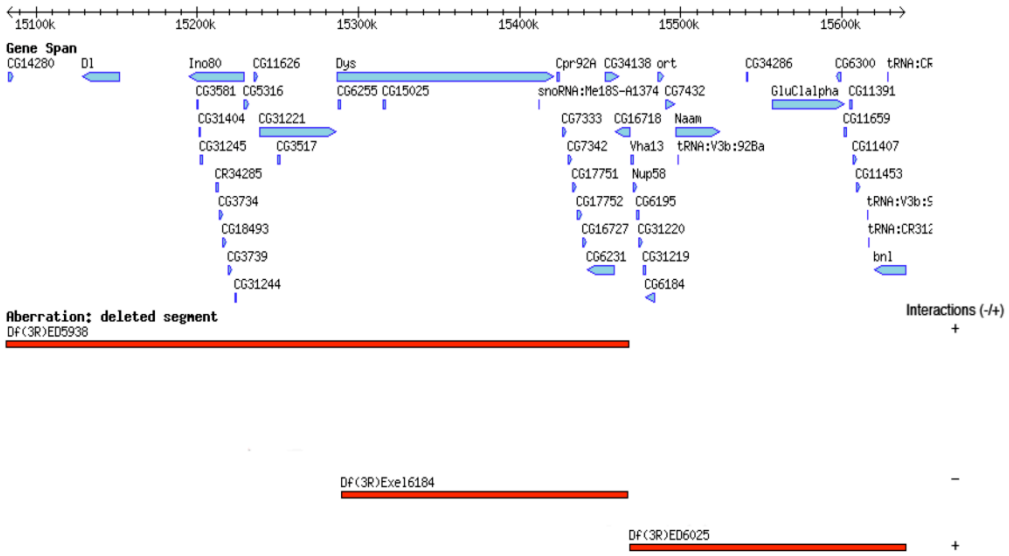

Figure 11. Within the region 3R:15082016..15638909, it was narrowed down to *CG16718*, a member of the Aberrent X segregation transmembrane protein family, as a candidate responsible for the strong dorsal-ventral defect.

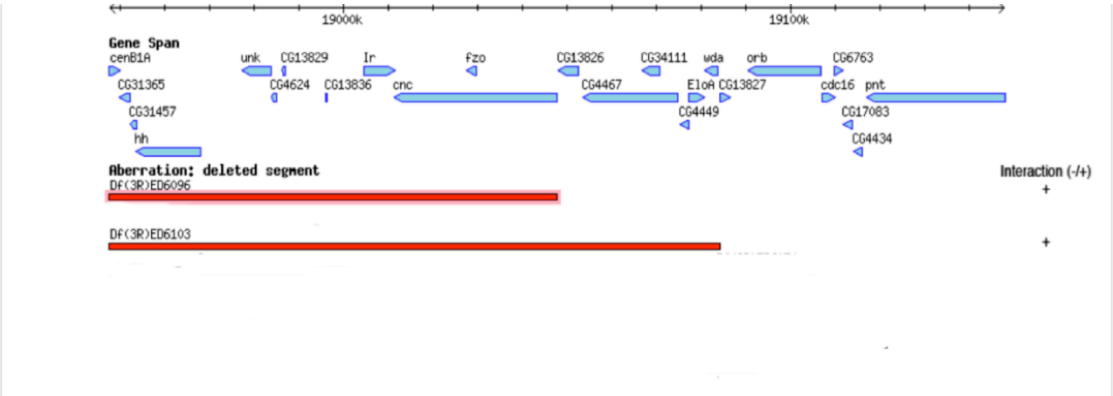

Figure 12. Gene span showing the genes and regions for the deficiency stocks for 3R:18947691..19147690. By analyzing the regions that resulted in dorsal appendage deects when crossed with the three alleles of *tral,* possible candidate genes could be identified.

Table 9. Possible genes that may interact with *tral* on chromosome three within the span of 3R:18947691..19147690.

Gene	Biochemical Function/Homolog
cenB1A	AFR GTPase activator activity
CG31365	Nucleic Acid binding
CG31456	
hh	Cell surface binding; protein binding
unk	Zinc ion binding; DNA binding
CG4624	Hydrogen-exporting ATPase activity; phosphorylative mechanism
CG13829	Unknown
CG13836	Unknown
Ir	Inward rectifier potassium channel activity
cnc	**Blastoderm segmentation, oocyte microtubule cytoskeleton polarization, bicoid mRNA localization, oocyte dorsal/ventral axis specification**
fzo	GTPase activity
CG13826	Unknown

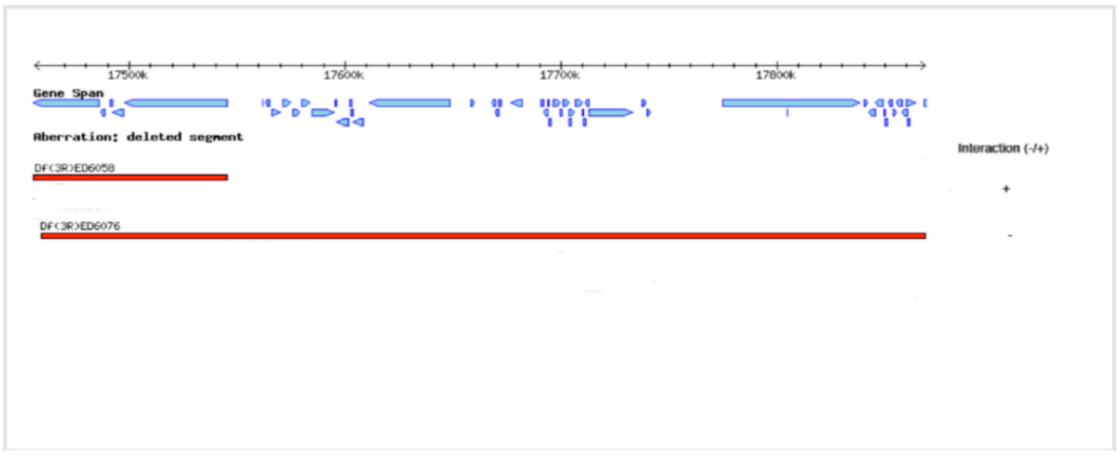

Figure 13. Gene span showing the genes and regions for the deficiency stocks for 3R:17456227..17,868,550. By analyzing the regions that resulted in dorsal appendage deects when crossed with the three alleles of *tral,* possible candidate genes could be identified.

Table 10. Possible genes that may interact with *tral* on chromosome three within the span of 3R:17456227..17,868,550.

Gene	Biochemical Function/Homolog
CG17991	Zinc ion binding
CG18766	Unknown
CG31063	Hydrolase activity
CG31064	Zinc ion binding
CG31065	Sodium channel activity
CG31068	Unknown
CG34006	Unknown
CG34293	Unknown
CG5984	Actin Binding
CG5987	Tubulin-tyrosine ligase activity
CG6051	Zinc ion binding
DNApol-alpha73	DNA-directed DNA polymerase activity
grass	Serine-type endopeptidase activity
Mdh	Malate dehydrogenase activity
pll	Protein domain specific binding
Ser	Protein binding
spn-D	DNA-dependent ATPase activity; germanium-derived oocyte fate determination
TFIIA-L	General RNA polymerase II transcription factor activity
woc	Regulation of transcription

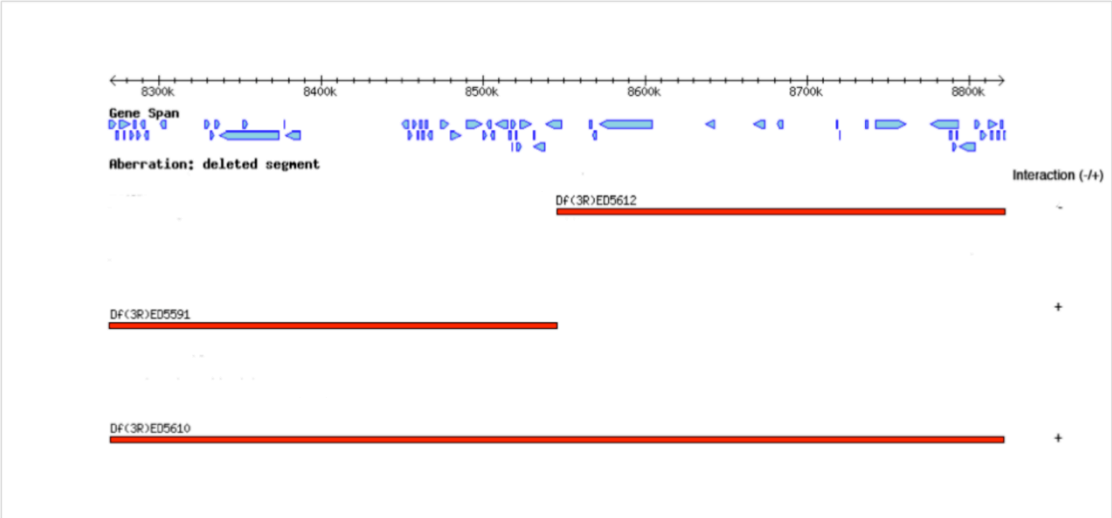

Figure 14. Gene span showing the genes and regions for the deficiency stocks for 3R:8,269,736..8,821,397. By analyzing the regions that resulted in dorsal appendage deects when crossed with the three alleles of *tral,* possible candidate genes could be identified.

Table 11. Possible genes that may interact with *tral* on chromosome three within the span of 3R:8,269,736..8,821,397.

Gene	Biochemical Function/Homolog
Alphagamma-element:CR32865	Unknown
Arp87C	Actin binding
CG11598	Lipase activity
CG11600	Triglyceride lipase activity
CG11608	Triglyceride lipase activity
CG12267	DNA-directed RNA polymerase activity
CG12279	Unfolded protein binding
CG14391	Unknown
CG14394	Unknown
CG14395	Unknown
CG18530	Triglyceride lipase activity
CG18616	Binding
CG18549	Unknown
CG31347	Unknown
CG33929	Unknown
CG5509	Unknown
CG5538	Unknown
CG31347	Unknown
CG33929	Unknown
CG6188	Glycine N-methyltransferase activity
CG6225	Aminopeptidase activity
CG6234	Unknown
CG6359	Protein binding
CG6753	Triglyceride lipase activity
Cyp313a4	Electron carrier activity
desat1	Stearoyl-coA-9-desaturase activity
kar	Ommochrome biosynthetic process
Mir-284	Unknown
Hsp70Ba	ATP binding
Hsp70Bb	ATP binding
Hsp70Bc	ATP binding
hug	Receptor binding
mus308	DNA repair
Octbeta2R	Octopamine receptor activity
Octbeta3R	Octopamine receptor activity
Past1	Endocytosis
Su(fu)	Transcription factor binding
Trus	Unknown
Vha55	Proton transport

CONCLUSION/FUTURE EXPERIMENTS

A genetic screen was performed to isolate genes on the third chromosome of *Drosophila melanogaster* that interact with *tral.* Four genes were identified by mapping the deficienes to a single gene to determine possible candidates for interaction with *tral* through crosses between chromosome three deficiencies and three *tral* mutant alleles.

One of the candidate genes was *stg,* a gene known to regulate the mitotic cycle. However, upon crossing a null mutant of *stg* with *tral*, the dorsal appendage deficiency defect originally seen was no longer present. As a result, it was concluded that the original data collected may have been a false positive result. Another possible conclusion from this data is that *stg* does not interact directly with *tral* but rather disrupts *grk* expression due to disruption in the Cdk2/CycE complex thereby affecting the dorsal-ventral patterning mechanism. The dorsal appendage defect originally seen in the broader deficiency cross was not seen when a null mutation of *stg* was crossed with the three alleles of *tral.* An explanation for this lack of interactions could be that there is another candidate gene that has not yet been identified in this region or there are mobile elements or enhancers that are disrupted which will in turn affect the expression of the gene when a null mutation of *stg* is crossed with *tral.* An experiment that can be done to confirm this hypothesis is to see where *grk* mRNA localizes to in a null mutation of *stg.* If the localization has a different expression from a *stg/tral* mutant, then *grk* expression is disrupted. *tral* affects *grk* secretion, but if *grk*

expression is disrupted, then *stg* does not necessarily have to interact with *tral* as *grk* secretion and expression are mutually exclusive.

The second candidate gene thought to interact with *tral* was CG16718, an Axs-like protein. Through *in situ* experiments of the CG16718 gene, mRNA could not be detected due to high background noise. We could not conclude where the mRNA localizes, and therefore could not determine how CG16718 interacts with *tral.* Mutations in the Axs gene leads to disruption in spindle formation hindering the proper secretion of the mRNAs in the oocyte to establish polarity. Because *osk* yw was localized posteriorly, we know that the procedures were done correctly but that the amount of mRNA was too low for detection by *in situ* experiments. Future experiments could include qPCR in order to quantify and detect the message. In addition, a Northern Blot can be done to ensure that the RNA used for *in situ* experiments is the right size and correlates with the CG16718 RNA of interest.

A third gene that showed a positive interaction with *tral* was *cnc.* We set out to confirm published protein expression data and to test *cnc/tral* mutants to further understand the interaction between the two genes. When the oocytes were stained using immunofluorescence, there was little detectable Cnc protein seen in the mutant, which was similarly observed in the yw control. Future experiments including testing for proper Cnc protein expression via Western blot need to be performed. In addition, cDNA of cnc can be obtained and *in situ* and immunofluoresence experiments can be conducted to see if there is a difference in the regulation of the Cnc protein in the mutant from that of the normal secretory pathway.

Finally, a fourth gene of interest was *pum*, a gene required for germline stem cell maintenance. Pum is part of a complex that represses translation and functions in the posterior body patterning in *Drosophila* embryos. In the absence of *pum* activity, somatic cells over-proliferate and form tumors, which supports the notion that *pum* is required for the maintenance of the germline stem cells. In order to insure that *pum* is the gene that interacts with *tral,* further experiments must be carried out. A null deficiency of *pum* can be crossed with the three alleles of *tral.* If strong dorsal appendage defect is detected, then *in situs* can be performed to determine the mRNA localization of *pum* and see if *pum* mutants have disrupted *grk* mRNA localization or *grk* secretion.

Another experiment that can be conducted to determine more genes that interact with *tral* is to complete the third chromosome deficiency screening. Although many deficiency stocks were crossed in this genetic screen, there were others available that could be crossed with *tral* to determine more specific regions and a more complete picture of all genes on the third chromosome that interact with *tral.*

Tral is an integral component required for the proper secretion of Grk and patterning in oogenesis. Clearly, understanding the interaction of this gene with other genes found on the third chromosome is important to understand its effect on the classical secretory pathway and efficient protein trafficking in the cell.

APPENDIX

CG16718 Primers

500 bp PCR product:

Forward Primer (5’ CGA TTT AGG TGA CAC TAT AGA GCA ACG CCC CCA CGC TC 3’)

Reverse Primer (5’ TAA TAC GAC TCA CTA TAG GGG ACG CTT TTG GTC GAT CGA TTG ACC ACG 3’)

REFERENCES

Bellen, H.J., Levis, R.W., Liao, G., He., Y., Carlson, J.W., Tsang, G., Evans-Holm, M., Hiesinger, P.R., Schulze, K.L., Rubin, G.M., et al. (2004). The BDGP gene disruption project: single transposon insertions associated with 40% of *Drosophila* genes. *Genetics, 167, 761-781.*

Ephrussi, A., Dickinson, L.K., and Lehmann R. (1991). *Oskar* organizes the germ plasm and directs localization of the posterior determinant nanos. *Cell, 66, 37-50.*

Forbes, A., and Lehmann, R. (1998). Nanos and Pmilio have critical roles in the development and function of *Drosophila* germline stem cells. *Development, 125, 679-690.*

Guichet, A., Peri, F., Roth, S. (2001). Stable anterior anchoring of the oocyte nucleus is required to establish dorsoventral polarity of the *Drosophila* egg. *Developmental Biology, 237,93-106.*

Jüschke, C., Ferring, D., Jansen, R., & Seedorf, M. (2004). A Novel Transport Pathway for a Yeast Plasma Membrane Protein Encoded by a Localized mRNA. *Current Biology, 14, 406-411.*

Kim-Ha, J., Smith, J.L., and Macdonald, P.M. (1991). o*skar* mRNA is localized to the posterior pole of the *Drosophila* oocyte. *Cell, 66, 23-35.*

Koch, E.A. & King, R.C. (2005). The origin and early differentitation of the egg chamber of *Drosophila melanogaster. Journal of Morphology, 119, 283-303.*

Kramer, G. & Hawley, R.S., (2003). The Spindle-associated transmembrane protein Axs identifies a membranous structure ensheating the meiotic spindle. *Nature, 5, 261-263.*

Macdonald, P.M., Geng, C. (2007). Identification of Genes tha Influence *gurken* Expression. *Fly, 5, 1-9.*

Macdonald, P.M. (1992). The *Drosophilia pumilio* gene: an unusually long transcription unit and an unusual protein. *Development, 114, 221-232.*

Martin, S., Leclerc, V., Smith-Litière, K., & St Johnston, D. (2003). The identification of novel genes required for *Drosophila* anteroposterior axis formation in a germline clone screen using GFP-Staufen. *Developmental, 130, 4201-4215.*

McGinnis, N., Ragnhildstveit, E., Veraksa, A., & McGinnis, W. (1998). A cap 'n' collar protein isoform constains a selective Hox repressor function. *Development*, *123, 4553-4564.*

Mohler, J., Mahaffey, J.W., Deutsch, E., & Vani, K. (1995). Control of Drosophila head segment identity by the bZIP homeotic gene cnc. *Development*, 121, 237-247.

Mohler, J., Vani, K., Leung, S., & Epstein, A. (1991). Segmentally restricted, cephalic expression of a leucine zipper gene during Drosophila embryogenesis. *Mech. Dev.*, *34, 3-9.*

Murata, Y. and Wharton, R.P. (1995). Binding of Pumilio to maternal *hunchback* mRNA is required for posterior patterning in *Drosophila* embryos. *Cell, 80, 747-756.*

Neuman-Silberberg, F.S., and Schupbach, T. (1993). The *Drosophila* TGF-α-like protein Gurken: expression and cellular localization during *Drosophila* oogenesis. *Mech. Development, 59, 105-113.*

Neuman-Silberberg, F.S., and Schupbach, T. (1993). The Drosophila dorsoventral patterning gene *gurken* produces a dorsally localized RNA and encodes a TGF-alpha-like protein. *Cell, 75, 165-174.*

O'Farrell, P.H., Edgar, B.A., Lakich, D. and Lehner, C.F. (1989). Directing cell division during development. *Science, 246, 635-640.*

Reed, B.H. (1995). *Drosophila* development pulls the strings of the cell cycle. *BioEssays, 17, 553-556.*

Riechmann, V., Ephrussi, A. (2001). Axis formation during Drosophila oogeneis. *Development, 11, 374-383.*

Spassov, D.S. and Jurecic, R. (2003). The PUF Family of RNA-binding Proteins: Does Evolutionarily conserved Structure Equal Conserved Function? *Life, 55, 359-366.*

Theurkarf, W.E., Smiley, S., Wong, M.L., and Albert, B.M. (1992). Reorganization of the cytoskeleton during *Drosophila* oogenesis implications for axis specification and intercellular transport. *Development, 115, 923-936.*

Wilhelm, J.E., Buszczak, M., & Sayles, S. (2005). Efficient Protein Trafficking Requires Trailer Hitch, a Component of a Ribonucleoprotein Complex Localized to the ER in *Drosophila. Developmental Cell, 9, 675-685.*

Wilhelm, J.E., Hilton, M., Amos, Q., Henzel, W.J. (2003). Cup is an eIF4E binding protein required for both the translational repression of oskar and the recruitment of Barentsz. *Cell Biology, 163, 1197-1204.*

Wilhelm, J.E., and Smibert, C.A. (2005). Mechanisms of translational regulation in *Drosophila*. *Cell, 97, 235-252.*

Xi., R., McGregor, J.R., & Harrison, D.A. (2003). A gradient of JAK pathway activity patterns the anterior-posterior axis of the follicular epithelium. *Developmental Cell, 4, 157-177.*

Yang YD, Cho H, Koo JY, Tak MH, Cho Y, Shim WS, Park SP, Lee J, Lee B, Kim BM, Raouf R, Shin YK, Oh U. (2008). TMEM16A confers receptor-activated calcium-dependent chloride conductance. *Nature, 455, 1210-1215.*